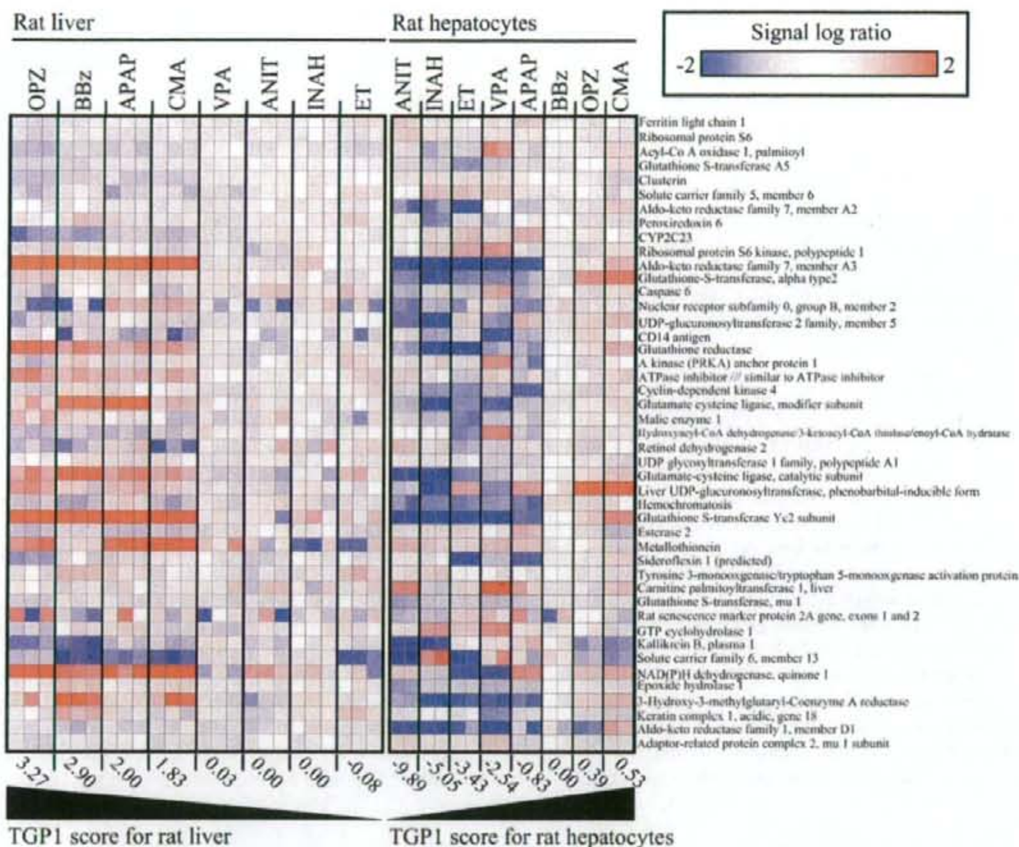

Fig. 7. Gene expression profile of glutathione deficiency-related genes.
The fold change value for each of the glutathione deficiency-related genes was calculated by dividing the signal value of chemical-treated rats or rat hepatocytes by the mean signal value of corresponding vehicle-treated rats (n=3) or rat hepatocytes (n=2), respectively, and the fold change values were converted to logarithm values where the base was set to 2. The heat map representing individual expression levels of glutathione deficiency-related genes was created using the logarithm values of fold changes.

ACKNOWLEDGMENT

This study was supported in part by a grant from the Ministry of Health, Labor and Welfare (H14-Toxico-001).

REFERENCES

Bichet, N., Cahard, D., Fabre, G., Remandet, B., Gouy, D. and Cano, J.P. (1990): Toxicological studies on a benzofuran derivative. III. Comparison of peroxisome proliferation in rat and human hepatocytes in primary culture. Toxicol. Appl. Pharmacol., **106**, 509-517.

Bock, K.W. and Kohle, C. (2005): Ah receptor- and TCDD-mediated liver tumor promotion: clonal selection and expansion of cells evading growth arrest and apoptosis. Biochem. Pharmacol., **69**, 1403-1408.

Boess, F., Kamber, M., Romer, S., Gasser, R., Muller, D., Albertini, S. and Suter, L. (2003): Gene expression in two hepatic cell lines, cultured primary hepatocytes, and liver slices compared to the *in vivo* liver gene expression in rats: Possible implications for toxicogenomics use of *in vitro* systems. Toxicol. Sci., **73**, 386-402.

Boverhof, D.R. and Zacharewski, T.R. (2006): Toxicogenomics in risk assessment: Applications and needs. Toxicol. Sci., **89**, 352-360.

Draghici, S. (2003): Analysis and visualization tools. In Data Analysis Tools for DNA Microarrays (Etheridge, A.M., Gross, L.J., Lenhart, S., Maini, P. K., Safer, H. M. and Voit, E. O., eds.), pp. 231-261. CRC Press, London.

Ellinger-Ziegelbauer, H., Stuart, B., Wahle, B., Bomann, W. and Ahr, H.J. (2004): Characteristic expression profiles induced by genotoxic carcinogens in rat liver. Toxicol. Sci., **77**, 19-34.

Gocke, E. (1996): Review of the genotoxic properties of chlorpromazine and related phenothiazines. Mutat. Res., **366**, 9-21.

Gonzalez, F.J., Peters, J.M. and Cattley, R.C. (1998): Mechanism of action of the nongenotoxic peroxisome proliferators: Role of the peroxisome proliferator-activator receptor alpha. J. Natl. Cancer Inst., **90**, 1702-1709.

Iatropoulos, M.J., Williams, G.M., Abdo, K.M., Kari, F.W. and Hart, R.W. (1997): Mechanistic studies on genotoxicity and carcinogenicity of salicylazosulfapyridine an anti-inflammatory medicine. Exp. Toxicol. Pathol., **49**, 15-28.

Ito, K., Kiyosawa, N., Kumagai, K., Manabe, S., Matsunuma, N. and Yamoto, T. (2006): Molecular mechanism investigation of cycloheximide-induced hepatocyte apoptosis in rat livers by morphological and microarray analysis. Toxicology, **219**, 175-186.

James, L.P., Mayeux, P.R. and Hinson, J.A. (2003): Acetaminophen-induced hepatotoxicity. Drug Metab. Dispos., **31**, 1499-1506.

Kaminski, N. and Friedman, N. (2002): Practical approaches to analyzing results of microarray experiments. Am. J. Respir. Cell Mol. Biol., **27**, 125-132.

Kiyosawa, N., Ito, K., Sakuma, K., Niino, N., Kanbori, M., Yamoto, T., Manabe, S. and Matsunuma, N. (2004a): Evaluation of glutathione deficiency in rat livers by microarray analysis. Biochem. Pharmacol., **68**, 1465-1475.

Kiyosawa, N., Tanaka, K., Hirao, J., Ito, K., Niino, N., Sakuma, K., Kanbori, M., Yamoto, T., Manabe, S. and Matsunuma, N. (2004b): Molecular mechanism investigation of phenobarbital-induced serum cholesterol elevation in rat livers by microarray analysis. Arch. Toxicol., **78**, 435-442.

Lake, B.G., Gray, T. J., Evans, J.G., Lewis, D.F., Beamand, J.A. and Hue, K.L. (1989): Studies on the mechanism of coumarin-induced toxicity in rat hepatocytes: Comparison with dihydrocoumarin and other coumarin metabolites. Toxicol. Appl. Pharmacol., **97**, 311-323.

Lehmann, J.M., Lenhard, J.M., Oliver, B.B., Ringold, G.M. and Kliewer, S.A. (1997): Peroxisome proliferator-activated receptors alpha and gamma are activated by indomethacin and other non-steroidal anti-inflammatory drugs. J. Biol. Chem., **272**, 3406-3410.

Liu, G., Loraine, A.E., Shigeta, R., Cline, M., Cheng, J., Valmeekam, V., Sun, S., Kulp, D. and Siani-Rose, M.A. (2003): NetAffx: Affymetrix probesets and annotations. Nucleic Acids Res., **31**, 82-86.

Martelli, A., Mattioli, F., Mereto, E., Brambilla Campart, G., Sini, D., Bergamaschi, G. and Brambilla, G. (1998): Evaluation of omeprazole genotoxicity in a battery of *in vitro* and *in vivo* assays. Toxicology, **130**, 29-41.

Morii, M., Takata, H. and Takeguchi, N. (1989): Acid activation of omeprazole in isolated gastric vesicles, oxyntic cells, and gastric glands. Gastroenterol., **96**, 1453-1461.

Peters, J.M., Cattley, R.C. and Gonzalez, F.J. (1997): Role of PPAR alpha in the mechanism of action of the nongenotoxic carcinogen and peroxisome proliferator Wy-14,643. Carcinogenesis, **18**, 2029-2033.

Richert, L., Lamboley, C., Viollon-Abadie, C., Grass, P., Hartmann, N., Laurent, S., Heyd, B., Mantion, G., Chibout, S.D. and Staedtler, F. (2003): Effects of clofibric acid on mRNA expression profiles in primary cultures of rat, mouse and human hepatocytes. Toxicol. Appl. Pharmacol., **191**, 130-146.

Sawada, H., Takami, K. and Asahi, S. (2005): A toxicogenomic approach to drug-Induced phospho-

lipidosis: Analysis of its induction mechanism and establishment of a novel *in vitro* screening system. Toxicol. Sci., **83**, 282-292.

Sehata, S., Kiyosawa, N., Makino, T., Atsumi, F., Ito, K., Yamoto, T., Teranishi, M., Baba, Y., Uetsuka, K., Nakayama, H. and Doi, K. (2004): Morphological and microarray analysis of T-2 toxin-induced rat fetal brain lesion. Food Chem. Toxicol., **42**, 1727-1736.

Smith, A.G., Francis, J.E., Dinsdale, D., Manson, M.M. and Cabral, J.R. (1985): Hepatocarcinogenicity of hexachlorobenzene in rats and the sex difference in hepatic iron status and development of porphyria. Carcinogenesis, **6**, 631-636.

Szymanska, J.A. (1996): Biochemical alterations as measures of acute and subacute hepatotoxicity of 1,3-dibromobenzene in rat. Arch. Toxicol., **71**, 99-106.

Takashima, K., Mizukawa, Y., Morishita, K., Okuyama, M., Kasahara, T., Toritsuka, N., Miyagishima, T., Nagao, T. and Urushidani, T. (2006): Effect of the difference in vehicles on gene expression in the rat liver-analysis of the control data in the Toxicogenomics Project Database. Life Sci., **78**, 2787-2796.

Urushidani, T. and Nagao, T. (2005): Toxicogenomics: The Japanese initiative. In Handbook of Toxicogenomics - Strategies and Applications (Borlak, J., ed.), pp. 623-631. Wiley - VCH.

Weidolf, L., Karlsson, K.E. and Nilsson, I. (1992): A metabolic route of omeprazole involving conjugation with glutathione identified in the rat. Drug Metab. Dispos., **20**, 262-267.

The Journal of Toxicological Sciences,
Vol.31, No.5, 449-469, 2006

COMPARISON OF GENE EXPRESSION PROFILES AMONG PAPILLA, MEDULLA AND CORTEX IN RAT KIDNEY

Kotaro TAMURA[1], Atsushi ONO[1], Toshikazu MIYAGISHIMA[1],
Taku NAGAO[2] and Tetsuro URUSHIDANI[1,3]

[1]*Toxicogenomics Project, National Institute of Biomedical Innovation,*
7-6-8 Saito-Asagi, Ibaraki, Osaka 567-0085, Japan
[2]*National Institute of Health Sciences,*
1-18-1 Kamiyoga, Setagaya-Ku, Tokyo 158-8501, Japan
[3]*Department of Pathophysiology, Faculty of Pharmaceutical Sciences,*
Doshisha Women's College of Liberal Arts, Kodo, Kyotanabe, Kyoto 610-0395, Japan

(Received August 18, 2006; Accepted September 11, 2006)

ABSTRACT — The aim of this study was to compare gene expression profiles in the different kidney regions as the basis for toxicogenomics. Rat kidney was separated into papilla, medulla and cortex, and total RNA was isolated from these and from the whole slice. Gene expression profiling was performed using Affymetrix Rat Genome 230 2.0 Array. When global normalization was applied, the expression of β-actin or GAPDH varied among the regions. It was considered that such a comparison could not be made, especially between papilla and other portions, since the production of total mRNA in the former was relatively low. In fact, ANOVA was performed on the gene expression values with global normalization in papilla, medulla, cortex, and whole slice, and the numbers of genes appeared to be the highest in papilla. It was also observed that many genes showed their maximum or minimum in the whole slice, which was theoretically impossible. To overcome the problems associated with global normalization, the "percelome" normalization (a way to obtain the values directly related to the copies of mRNA per cell) was employed to compare the regions. In applying this procedure, probe sets with regional difference in expression were efficiently extracted by ANOVA. When they were sorted by the fold difference to other regions, the higher rank was occupied by genes characteristic of the functions of kidney, i.e., channels, transporters and metabolic enzymes. Some of them were consistent with the literature and were related to pathophysiological phenomena. Comprehensive comparison of data of gene expression in the renal anatomical area will greatly enhance studies of the physiological function and mechanism of toxicity in kidney.

KEY WORDS: Toxicogenomics, Kidney, Gene expression, Regional difference, Rat

INTRODUCTION

The Toxicogenomics Project is a 5-year collaborative project by the National Institute of Health Sciences (NIHS) and 17 pharmaceutical companies in Japan which was started in 2002 (Urushidani and Nagao, 2005). In April 2005, some rearrangements were made and now the project is conducted by NIHS, the National Institute of Biomedical Innovation, and 15 pharmaceutical companies. Its aim is to construct a large-scale toxicology database of transcriptome for prediction of toxicity of new chemical entities in the early stage of drug development. About 150 chemicals, mainly medicinal compounds, have been selected, and the following are examined for each. The *in vivo* test using rat consists of a single administration test (3, 6, 9 and 24 hr with 4 dose levels including vehicle control) as well as a repeated administration test (3, 7, 14 and 28 days with 4 dose levels including vehicle control), and then data of body weight, general symptoms, histopathological examination of liver and kidney, and blood biochemistry are obtained from each animal. Gene

Correspondence: Tetsuro URUSHIDANI (E-mail: turushid@dwc.doshisha.ac.jp)

expression in liver (and kidney in some cases) is comprehensively analyzed by using Affymetrix GeneChip. An *in vitro* test using rat and human hepatocytes is also carried out to accomplish the bridging between the species. Although the main target of the project is liver, about 10 of the chemicals are typical nephrotoxicants and many others exhibited nephrotoxicity in addition to hepatotoxicity. In our project, we plan to perform gene expression analysis of kidney for up to 30 such chemicals.

Although the toxicogenomics technique is established as a powerful tool for prediction of nephrotoxicity of drugs (Thukra *et al.*, 2005), it is well known that kidney consists of a variety of cell types and that the physiological functions, including gene expression, differ between the anatomical portions, i.e., papilla, medulla, and cortex. Therefore, we expected that different gene expression profiles would be obtained either when kidney is analyzed as a whole or separated into each portion. For an exploratory test, we checked potential region-related differences in gene expression before starting analysis of drug effects on the kidney.

In employing global normalization, based on the assumption that the total amount of mRNA is constant, it can cause a bias in the comparison of the different portions, since the rate of transcription varies with the cell types. In our project, gene expression values can be converted to a value proportional to the copies of mRNA per cell (the values normalized by externally adding standard mRNA in an amount proportional to the DNA content in the homogenate) by employing a system, "percellome" (Kanno *et al.*, 2006). In the present study, quantification by this system was compared to that of global normalization.

MATERIALS AND METHODS

Animals and Sampling

Male Sprague-Dawley rats were purchased from Charles River Japan Inc., (Kanagawa, Japan) at 5-weeks of age. After a 7-day quarantine and acclimatization period, 6 of the animals were euthanized by exsanguination from the abdominal veins and arteries under ether anesthesia. Kidneys were collected from each animal, and sliced horizontally at its middle portion with ca. 1 mm thickness by a pair of razor blades with a spacer in between. The slice was put into RNA later (Ambion, Austin, TX, USA) overnight for expression profiling. The fixed slices from three (No. 1 to 3) out of 6 animals were then separated into papilla, medulla, and cortex, as shown in Fig. 1. The remaining three (No. 4 to 6) were analyzed as a whole slice. The experimental protocols were reviewed and approved by the Ethics Review Committee for Animal Experimentation of the National Institute of Health Sciences.

Expression profiling

The kidney samples (whole slice, papilla, medulla and cortex) were homogenized using Mill Mixer (Qiagen) and zirconium beads. Total RNA was isolated from the kidney homogenate using RNeasy kit. Purity of the RNA was checked by gel electrophoresis, and the 260/280 nm ratio was between 2.0-2.2. Microarray analysis was conducted on 3 samples for each group by using GeneChip Rat Genome 230

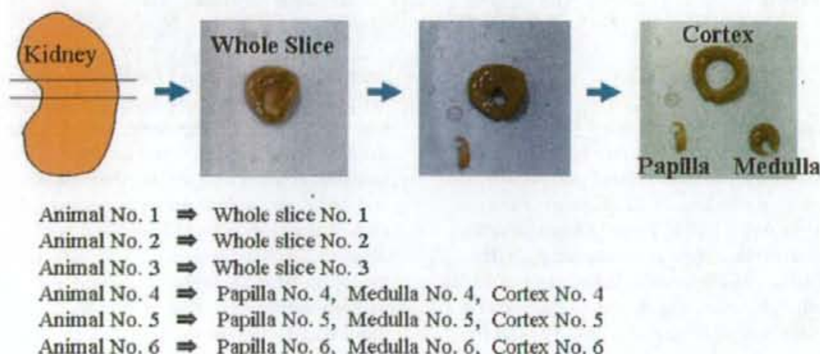

Fig. 1. Sampling and preparation of kidney for GeneChip analysis.

2.0 Arrays (Affymetrix, Santa Clara, CA, USA) containing 31,099 probe sets. The procedure was basically conducted according to the manufacturer's instructions using Superscript Choice System (Invitrogen, Carlsbad, CA, USA) and T7-(dT)24-oligonucleotide primer (Affymetrix) for cDNA synthesis, cDNA Cleanup Module (Affymetrix) for purification, and IVT Labeling Kit (Affymetrix) for synthesis of biotin-labeled cRNA. Twenty μg of the fragmented cRNA was hybridized to a Rat Genome 230 2.0 Array for 18 hr at 45°C at 60 rpm after which the array was washed and stained by streptavidin- phycoerythrin using Fluidics Station 450 (Affymetrix) and then scanned by Gene Array Scanner (Affymetrix).

Percellome normalization

We primarily use global mean normalization for data analysis in our project. However, to compare a sample from a different kidney region, in which the activity of transcription might be different, global normalization based on the total mRNA appeared not to provide the correct result. In the present study, we employed "percellome normalization" to normalize data as well.

The Percellome method reported by Kanno *et al.* (2006) was shown to be effective to compare the data from different tissues or different platform. In this method, the grade-dosed spike cocktail (GSC), which consists of five different Bacillus subtilis mRNA with different concentrations, was added to the tissue homogenate in proportion to its DNA contents before RNA extraction, assuming that all the cells contain a fixed amount of genomic DNA (g/cell) across the samples. The copy number of the RNA in one cell was calculated from the function of signal values of GSC and their copy number. Therefore, the effect of the difference in the total gene expression between samples can be avoided and a direct comparison of the expression data of samples from different sources is enabled.

The GSC used in this study was generously provided by Dr. Kanno, and the experimental procedure and calculations of the percellome method was conducted according to the original procedure. By separate experiments, we confirmed that GSC did not affect signals of other RNA and that the effect on global mean value was negligible.

Statistical Analysis

The data was analyzed by using GeneSpring version 6.1 (Silicon Genetics, Santa Clara, CA, USA), 2003 (Microsoft, Redmond, WA, USA) and MeV version 3.1 (The Institute for Genomic Research, Rockville, MD, USA). Expression data were customarily normalized using the mean value, multiplied by 500 (global mean normalization). Filtering of the data was performed either by flags (present, absent and marginal call) or ANOVA (Snedecor and Cochran, 1989).

RESULTS

First, analyses were conducted by our routine procedure, global normalization, in which each signal intensity was divided by the mean of each chip and multiplied by an arbitrary number to adjust the mean of each to the same value. In order to check the efficacy of the normalization procedure, the values of β-actin and GAPDH in each sample were divided by the mean value of the total 12 samples (Table 1). Expressed by this number, the values of β-actin varied between 0.91 - 0.99 in papilla, 0.98 - 1.12 in medulla, 0.97 - 1.14 in cortex, and 0.94 - 1.04 in the whole slice, resulting in an overall range of 0.91 - 1.14 (25% variation). The expression of GAPDH varied 0.76 - 0.85 in papilla, 1.01 - 1.05 in medulla, 1.11 - 1.19 in cortex, and 1.02 - 1.04 in the whole slice, resulting in an overall range of 0.76 - 1.19 (50% variation). Although they are relatively close to 1 (the mean value was 0.94, 1.02, and 1.03 for β-actin and 0.81, 1.03 and 1.16 for GAPDH in papilla, medulla, and cortex, respectively), the differences seemed to be too large to be ignored.

Using the data analyzed with global normalization, Pearson's correlation was calculated for each pair of the samples and is shown in Table 2A. The correlation coefficients were quite high among 3 samples from the same region, i.e., all were larger than 0.985. The correlation between papilla and others were lower than that between medulla and cortex, i.e., 0.821 - 0.860 between papilla and medulla, 0.741 - 0.789 between papilla and cortex, whereas it was 0.936 - 0.955 between medulla and cortex. The correlation coefficients between each of the three regions and the whole slice were in this order: cortex (0.981 - 0.987) > medulla (0.954 - 0971) > papilla (0.770 - 0.814), suggesting that gene expression in the whole slice preferentially represents that in cortex but it does not well represent that in papilla.

To try to identify genes with differential expression in the three regions, we first used a parameter of GeneChip data, detection call (present, marginal, and absent). Probe sets with present call in all samples in a region but all absent in other regions were selected as region-specific genes (Fig. 2). Genes with present call

Table 1. Signal intensity of β-actin and GAPDH.

Value type	Gene Title	Papilla			Medulla			Cortex			Whole		
		No.1	No.2	No.3	No.1	No.2	No.3	No.1	No.2	No.3	No.1	No.2	No.3
Signal intensity	β-actin	19619	20290	18700	20158	22911	20379	19881	23365	20759	19277	19278	21390
	GAPDH	17008	16029	15284	20169	21086	20291	22338	23834	23006	20765	20430	20458
Signal intensity Mean of signal intensity	β-actin	0.95	0.98	0.90	0.98	1.11	0.99	0.96	1.13	1.00	0.93	0.93	1.03
	GAPDH	0.85	0.81	0.77	1.01	1.06	1.02	1.12	1.20	1.16	1.04	1.03	1.03

Expression of β-actin and GAPDH in the three portions of kidney slice, papilla, medulla, and cortex, from three different rats (No. 1 - 3) as well as in the whole slice of three different rats (No. 4 - 6). Signal intensity of each gene was divided by the mean of all probes in the chip multiplied by 500 (global mean normalization, upper columns), after which each value was divided by the mean of these 12 values (per gene normalization).

in all samples of papilla but absent in all of medulla and cortex were 448, and only 27 (6%) were all present in the whole slice. Genes with present call in all samples of medulla but absent in others were quite rare, i.e., 18 probe sets, of which 2 (11%) had present call in all of the whole slices. Cortex-specific probes were found to be 44, and 34 (77%) were present in all of the samples of the whole slice. The relatively small number in the latter two portions indicates that most of the genes are common between medulla and cortex, and the gene expression in papilla is unique. These results suggest again that the region specific genes (in other than cortex) are difficult to detect by analysis of the whole slice.

The above results clearly indicate that the population of genes expressed in each region is quite different. Theoretically, absolute values of expression should be used when an accurate comparison is made between regions with different total mRNA contents. In order to further elucidate this point, the "percellome procedure" was employed to compare with global normalization.

The mean of copy numbers (or the values directly related to copy numbers) of β-actin was calculated to be 234, 291, 341, and 309 in papilla, medulla, cortex and the whole slice, respectively, i.e., the ratio in papilla, medulla, and cortex (whole slice = 1) was 0.76, 0.94 and 1.10, respectively. The mean of copy numbers of GAPDH was calculated to be 208, 298, 369 and 343, in papilla, medulla, cortex and the whole slice, respectively, i.e., the ratio in papilla, medulla, cortex (whole slice = 1) was 0.61, 0.87 and 1.08, respectively. These

Table 2. Pearson's correlation coefficient between samples.

A		Papilla			Medulla			Cortex			Whole		
		No1	No2	No3	No1	No2	No3	No1	No2	No3	No4	No5	No6
Papilla	No1	1	0.989	0.986	0.847	0.843	0.837	0.765	0.758	0.761	0.814	0.811	0.812
	No2		1	0.985	0.853	0.853	0.846	0.778	0.773	0.775	0.827	0.825	0.825
	No3			1	0.815	0.812	0.811	0.738	0.73	0.735	0.789	0.785	0.786
Medulla	No1				1	0.994	0.991	0.947	0.933	0.937	0.958	0.967	0.956
	No2					1	0.991	0.943	0.935	0.938	0.957	0.968	0.955
	No3						1	0.953	0.943	0.953	0.964	0.972	0.962
Cortex	No1							1	0.991	0.992	0.986	0.983	0.986
	No2								1	0.991	0.983	0.979	0.984
	No3									1	0.984	0.98	0.985
Whole	No4										1	0.996	0.994
	No5											1	0.992
	No6												1

B		Papilla			Medulla			Cortex			Whole		
		No1	No2	No3	No1	No2	No3	No1	No2	No3	No4	No5	No6
Papilla	No1	1	0.989	0.985	0.837	0.833	0.826	0.755	0.755	0.752	0.801	0.797	0.801
	No2		1	0.982	0.843	0.844	0.834	0.768	0.769	0.764	0.813	0.81	0.814
	No3			1	0.801	0.798	0.795	0.725	0.723	0.724	0.771	0.766	0.77
Medulla	No1				1	0.994	0.991	0.946	0.934	0.937	0.957	0.967	0.955
	No2					1	0.991	0.942	0.936	0.937	0.956	0.967	0.954
	No3						1	0.953	0.945	0.953	0.963	0.971	0.961
Cortex	No1							1	0.992	0.992	0.987	0.984	0.986
	No2								1	0.992	0.986	0.982	0.986
	No3									1	0.985	0.981	0.985
Whole	No4										1	0.996	0.994
	No5											1	0.992
	No6												1

Legend (shading): 0.90 – ; 0.85 – ; 0.80 – ; 0.75 – ; – 0.75

A: Calculated on the data of global normalization.
B: Calculated on the data of percellome.

values clearly differ from those by global normalization, namely, the expression values in papilla were apparently overestimated by global normalization. The correlation coefficients calculated from the values normalized by percellome (Table 2B) were almost identical to that in Table 2A except between papilla and others, which showed a relatively large decrease in value. These results again indicated that global normalization was problematic, especially for papilla among the portions, most possibly because of the low amount of mRNA production in that region, compared with others.

After normalization either by global mean or percellome, the genes with absent call in all the samples were discarded and analyzed by ANOVA ($p<0.01$) in order to extract probe sets showing different expression in any region(s). The numbers of extracted probe sets were 12,322 for percellome and 8,161 for global normalization. Fig. 3 shows the results of K-means clustering (Euclidean, 10 clusters) of the expression values converted into z-scores in order to see the trend of expression in each region.

By percellome normalization (Fig. 3A), clusters of probe sets with characteristic region-dependent expression were efficiently extracted. It was also obvious from the figure that there was only one cluster containing only 293 probe sets that showed specifically high expression in papilla, and the other probe sets showed the lowest value in papilla compared to any other clusters. This indicates that most of the probe sets showed the lowest expression in papilla and the highest ones were exceptional. On the other hand, the clusters of global normalization (Fig. 3B) showed various, inconsistent patterns. Contrasting with the case of percellome normalization, there were many clusters in which gene expression was highest in papilla, or where papilla was equivalent to other region(s).

An obvious contradiction was noted between the two normalizations as described above, so further comparison was made. After the elimination of the probe sets that had absent call in all samples, the probe sets were classified into categories where the values showed maximum or minimum. Fig. 4 shows their counts in papilla, medulla, cortex, and whole slice for each normalization method. In the case of percellome normalization (A), the numbers of probe sets showing a maximal value were dominantly found in cortex, while the most of those showing a minimum were in papilla. On the other hand, in the case of global normalization (B), many of the probe sets showing their maximum were in papilla, while the numbers of probe sets with minimal expression were distributed evenly among the samples. It is noteworthy that very many (>3,000) probe sets showed minimal expression in the whole slice. However, this is theoretically impossible because the whole slice contains all the other 3 portions. Therefore, it should be concluded that the extraction of the genes with region-specific expression based on global normalization gives an error, and thus percellome normalization should be used in this case.

Based on the above results, region-specific genes in kidney were extracted as follows. After selection by ANOVA ($p<0.01$) for the data of percellome normalization, genes were categorized by the position at which they showed the larger expression value and then aligned in the order of their ratio to the minimum, for papilla (Table 3), medulla (Table 4) and cortex (Table 5). As is obvious from Figs. 3 and 4, the production of mRNA per cell was considered to be in the order of cortex>medulla>papilla, and the numbers of region-specific probe sets were also in this order. For simplicity, probe sets without any annotation were eliminated, and the ones with the ratio of >3 for papilla, >10 for medulla, and >30 for cortex, are presented in the tables.

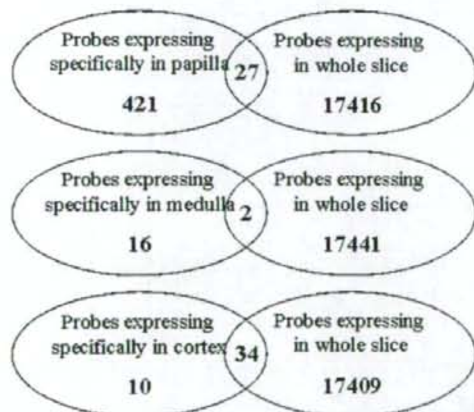

Fig. 2. Venn diagram of region-specific genes extracted by flags (present, absent and marginal call). The probes having "present call" in all samples of papilla and "absent call" in all samples of medulla and cortex were considered to be papilla-specific. The medulla- and cortex-specific probes were also extracted in the same manner and examined whether they were absent in the whole slice.

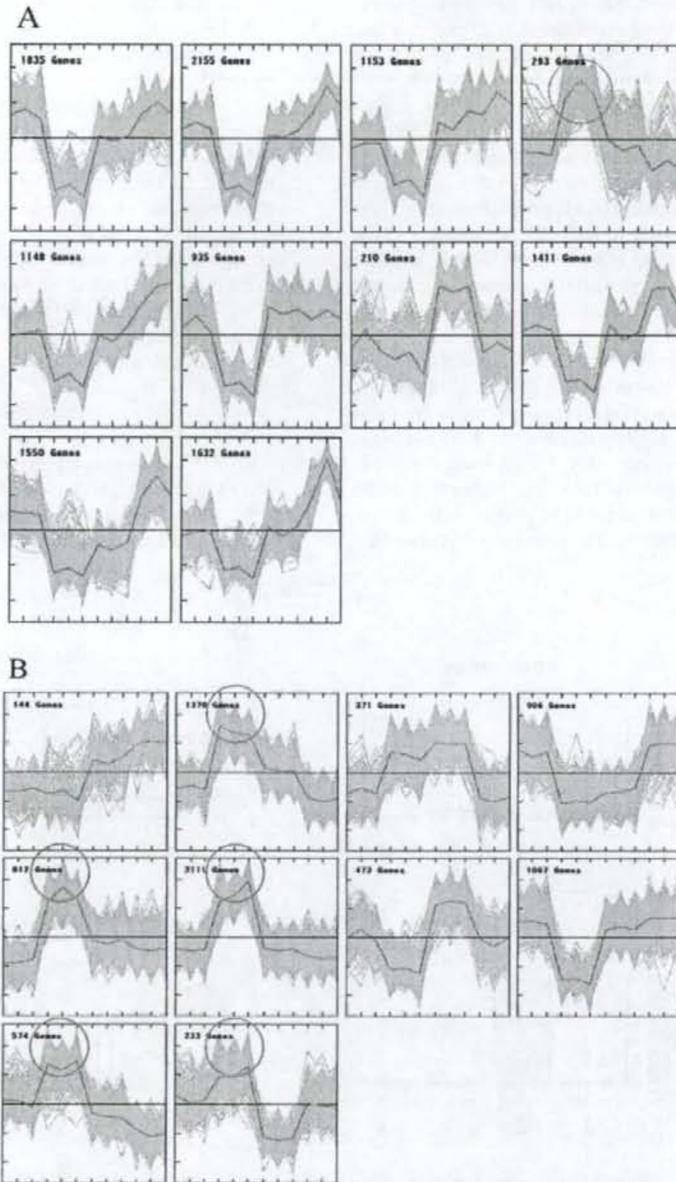

Fig. 3. K-means clustering of genes expressed in papilla, medulla, cortex, and whole slice of kidney. Data were processed by percellome normalization (A) or global mean normalization (B), and then converted into z-scores. K-means clustering (Euclidean, 10 clusters) was performed with MeV version 3.1 (The Institute for Genomic Research, Rockville, MD, USA). In each cluster, individual samples are aligned from left to right: whole slice (3), papilla (3), medulla (3), and cortex (3). Red lines indicatethe mean of the probes within each cluster. Orange circles indicate where papilla showed specifically high expression values.

In all these three tables, the higher rank is generally occupied by the genes related to channels, transporters and metabolic enzymes, suggesting that the gene lists are meaningful for analysis of specific renal functions.

In most of the papilla-enriched genes (Table 3), the ratio of papilla/cortex is larger than that of papilla/medulla, since the composition of papilla is closer to medulla than to cortex. The exceptional genes (highest in papilla and lowest in medulla) are shaded in the table. The outstanding feature of this table is that heat shock proteins and cytoskeleton/extracellular matrix proteins are present, in addition to the channel/transporters and metabolic enzymes.

In most of the medulla-enriched genes (Table 4), the ratio of medulla/cortex is less than 2, suggesting that their expression is relatively similar between these two portions. The genes with ratio of >3 are shaded in the table, but they are only 3 sets, indicating that medulla-specific genes are rare. The higher rank of the list in Table 4 is also occupied by channel/transporters and metabolic enzymes, and cytoskeletal proteins are scarce. A unique feature of medulla is the existence of 4 probe sets for prolactin receptor. This might occur simply because the quality of these multiple probes for one prolactin receptor is uniformly high.

Table 5 shows genes that showed the highest value in the cortex. It is noteworthy that many genes show more than 3 fold (shaded in the table) for the cortex/medulla ratio, indicating that there are many cortex-specific genes. The higher rank of this table is also occupied by channel/transporters and metabolic enzymes, but the numbers of metabolic enzymes are more prominent than in medulla.

Table 6 summarizes the genes categorized as channel/transporters, metabolic enzymes, cytoskeletons, and others for each portion.

DISCUSSION

The kidney is composed of various types of cells, and each portion (papilla, medulla, and cortex) has specific functions with wide variety, and the adverse effects of drugs vary with each portion. For example,

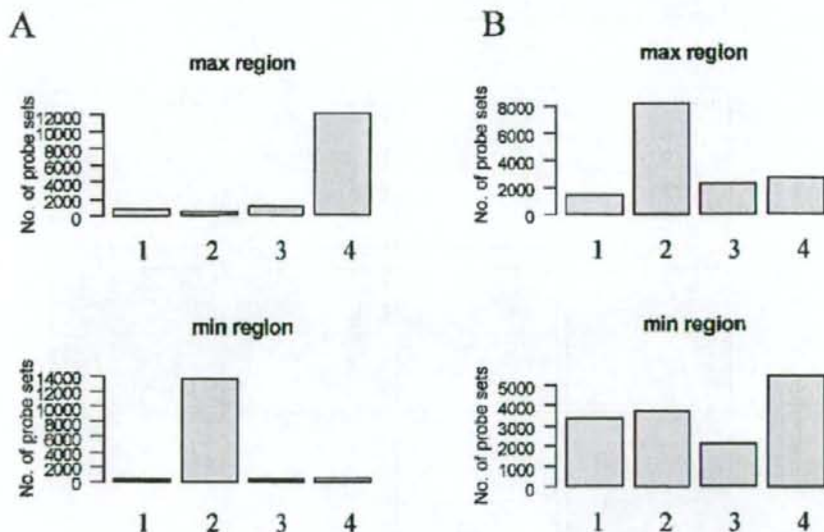

Fig. 4. The numbers of probe sets where their expression was maximal or minimal in whole slice, papilla, medulla, or cortex of kidney. After normalization by percellome (A) or global mean (B), probes with absent call in all samples were eliminated, and the numbers of probe sets with maximal (upper panels) or minimal (lower panels) were counted for each region, i.e., whole slice (1), papilla (2), medulla (3), and cortex (4).

Table 3. A list of probe sets specifically expressed in papilla of kidney.

Probe sets	papilla/ cortex	papilla/ medulla	medulla/ cortex	GENE_SYMBOL	GENE_NAME	channel transporter	Metabolic enzymes	cytoskeleton /extracellular matrix
1368259_at	32.0	12.7	2.5	Ptgs1	prostaglandin-endoperoxide synthase 1			
1389067_at	29.5	10.7	2.8	Slco4a1	solute carrier organic anion transporter family, member 4a1			
1372190_at	23.8	8.1	2.9	Aqp4	Aquaporin 4			
1394200_at	22.9	4.9	4.7	Hspa2	heat shock protein 2			
1387092_at	17.5	5.4	3.2	Fxyd4	FXYD domain-containing ion transport regulator 4			
1367847_at	17.4	5.4	3.2	Nupr1	nuclear protein 1			
1388460_at	16.8	5.6	3.0	Capg_predicted	capping protein (actin filament), gelsolin-like (predicted)			
1383469_at	7.2	14.6	0.5	Aldh1a3	Aldehyde dehydrogenase family 1, subfamily A3			
1376711_at	13.3	7.1	1.9	Cldn11	claudin 11			
1383319_at	13.2	2.5	5.3	Slc4a11_predicted	solute carrier family 4, sodium bicarbonate transporter-like, member 11 (predicted)			
1367734_at	13.1	7.9	1.7	Akr1b4	aldo-keto reductase family 1, member B4 (aldose reductase)			
1368765_at	10.7	2.5	4.2	Clcnk1	chloride channel K1			
1370229_at	10.5	1.9	5.4	Ndr4	N-myc downstream regulated 4			
1369841_at	10.3	4.2	2.4	Hspa2	heat shock protein 2			
1382303_at	3.8	8.8	0.4	RGD:1303187	phosphatase and actin regulator 1			
1378690_at	7.6	3.9	2.0	Ly6a_predicted	lymphocyte antigen 6 complex, locus A (predicted)			
1367661_at	6.8	3.7	1.8	S100a6	S100 calcium binding protein A6 (calcyclin)			
1374207_at	6.6	2.5	2.6	Agpt2	angiopoietin 2			
1369113_at	6.1	3.9	1.6	Grem1	gremlin 1 homolog, cysteine knot superfamily (Xenopus laevis)			
1368858_at	5.9	2.1	2.8	Ugt8	UDP-glucuronosyltransferase 8			
1368247_at	5.4	3.7	1.5	Hspa1a /// Hspa1b	heat shock 70kD protein 1A /// heat shock 70kD protein 1B			
1370334_at	3.2	5.4	0.6	Plekhb1	evectin-1			
1367650_at	5.1	3.1	1.6	Lcn7	lipocalin 7			
1374861_at	5.1	2.1	2.4	Tle2_predicted	transducin-like enhancer of split 2, homolog of Drosophila E(spl) (predicted)			
1387100_at	4.1	5.1	0.8	Aqp3	aquaporin 3			
1369949_at	5.0	3.6	1.4	Lu	Lutheran blood group (Auberger b antigen included)			
1369263_at	5.0	2.4	2.0	Wnt5a	wingless-type MMTV integration site 5A			
1370312_at	4.9	1.5	3.4	Spon1	spondin 1			
1388459_at	4.7	2.9	1.6	Col18a1	collagen, type XVIII, alpha 1			
1388456_at	4.3	3.0	1.4	S100a1	S100 calcium binding protein A1			
1393209_at	3.6	4.3	0.8	bsnd	Bartter syndrome, infantile, with sensorineural deafness (Barttin)			
1373733_at	4.3	2.8	1.5	Bok	Bcl-2-related ovarian killer protein			
1388547_at	4.2	2.5	1.7	Cldn4_predicted	claudin 4 (predicted)			

Table 3. Continued.

Probe sets	papilla/ cortex	papilla/ medulla	medulla/ cortex	GENE_SYMBOL	GENE_NAME	channel transporter	Metabolic enzymes	cytoskeleton /extracellular matrix
1396152_s_at	4.1	2.4	1.7	Igfbp5	insulin-like growth factor binding protein 5			
1367812_at	4.0	3.3	1.2	Spnb3	beta-spectrin 3			
1367577_at	3.4	3.9	0.9	Hspb1	heat shock 27kDa protein 1			
1372755_at	3.9	2.5	1.6	Mal2	mal, T-cell differentiation protein 2			
1370834_at	3.8	1.8	2.2	Hs3st1	heparan sulfate (glucosamine) 3-O-sulfotransferase 1			
1388155_at	3.8	3.3	1.2	Krt1-18	keratin complex 1, acidic, gene 18			
1372299_at	3.7	2.3	1.6	Cdkn1c	cyclin-dependent kinase inhibitor 1C (P57)			
1387886_at	3.6	2.7	1.3	Prelp	proline arginine-rich end leucine-rich repeat protein			
1368527_at	1.7	3.6	0.5	Ptgs2	prostaglandin-endoperoxide synthase 2			
1388102_at	1.9	3.5	0.5	Ltb4dh	leukotriene B4 12-hydroxydehydrogenase			
1370048_at	3.4	2.8	1.2	Edg2	endothelial differentiation, lysophosphatidic acid G-protein-coupled receptor, 2			
1371004_at	3.4	1.7	2.0	Sort1	sortilin 1			
1397830_at	3.4	2.3	1.5	Igfbp5	Insulin-like growth factor binding protein 5			
1369953_a_at	3.3	1.5	2.2	Cd24	CD24 antigen			
1367912_at	3.2	2.3	1.4	Ltbp1	latent transforming growth factor beta binding protein 1			
1387566_at	3.2	1.6	2.0	Pla2g4a	phospholipase A2, group IVA (cytosolic, calcium-dependent)			
1370912_at	3.2	2.3	1.4	Hspa1b	heat shock 70kD protein 1B			
1398318_at	3.2	2.1	1.5	Muc1	mucin 1, transmembrane			
1371625_at	3.1	2.8	1.1	Pygb	brain glycogen phosphorylase			
1370026_at	3.1	1.1	2.8	Cryab	crystallin, alpha B			
1393048_at	3.1	1.1	2.8	Adra2a	Adrenergic receptor, alpha 2a			
1388143_at	3.1	2.4	1.3	Col18a1	collagen, type XVIII, alpha 1			
1393958_at	3.1	2.1	1.5	Arhgap4	Rho GTPase activating protein 4			
1369084_a_at	3.1	2.8	1.1	Bok	Bcl-2-related ovarian killer protein			
1371499_at	3.0	1.8	1.7	Cd9	CD9 antigen			
1391830_at	3.0	1.9	1.6	Cpne8_predicted	copine VIII (predicted)			
1368342_at	3.0	1.9	1.6	Ampd3	adenosine monophosphate deaminase 3			
1384192_at	3.0	2.1	1.4	Chst1_predicted	carbohydrate (keratan sulfate Gal-6) sulfotransferase 1 (predicted)			
1398431_at	1.2	3.0	0.4	Car8_predicted	carbonic anhydrase 8 (predicted)			
1375170_at	3.0	1.6	1.9	S100a11_predicted	S100 calcium binding protein A11 (calizzarin) (predicted)			
1367759_at	3.0	1.2	2.5	H1f0	H1 histone family, member 0			
1387040_at	3.0	1.6	1.8	Mal	myelin and lymphocyte protein			

After selection by ANOVA ($p<0.01$) for the data of percellome normalization, genes maximally expressed in papilla were selected. The genes were aligned in the order of the ratio to the lower expression value, either in medulla or in cortex. As the genes listed here are expressed higher in medulla than cortex, in general, exceptional cases (ratio<0.6) are shaded in the medulla/cortex column. The genes categorized to "channel/transporters", "metabolic enzymes", or "cytoskeleton/extracellular matrix" are also shaded. Proteases or enzymes involving signal transduction are not included in the category of "metabolic enzymes". For simplicity, genes with less than 3-fold specificity are omitted.

Table 4. A list of probe sets specifically expressed in medulla of kidney.

Probe sets	medulla/ papilla	cortex/ papilla	medulla/ cortex	GENE_SYMBOL	GENE_NAME	channel transporter	Metabolic enzymes	cytoskeleton /extracellular matrix
1370377_at	204.8	124.5	1.6	Cyp2d9 /// Cyp2d10	cytochrome P450, family 2, subfamily d, polypeptide 9 /// cytochrome P450, family 2, subfamily d, polypeptide 10			
1387567_at	184.9	119.7	1.5	Slc21a1 /// LOC497799	solute carrier family 21, member 1 /// hypothetical gene supported by NM_017111			
1369401_at	153.0	69.6	2.2	Slc21a13	solute carrier family 21, member 13			
1387328_at	149.6	100.5	1.5	Cyp2c	Cytochrome P450, subfamily IIC (mephenytoin 4-hydroxylase)			
1368288_at	147.9	90.7	1.6	Gc	group specific component			
1368498_a_at	147.3	102.7	1.4	RGD:621387	kidney specific organic anion transporter			
1386454_at	133.0	46.7	2.8	Slc23a3_predicted	solute carrier family 23 (nucleobase transporters), member 3 (predicted)			
1370789_a_at	132.6	91.8	1.4	Prlr	prolactin receptor			
1387987_at	120.1	43.9	2.7	Slc22a19	solute carrier family 22 (organic anion transporter), member 19			
1390569_at	117.4	74.7	1.6	RGD:1359493	similar to carnosinase 1			
1369450_at	114.9	92.3	1.2	UST5r	integral membrane transport protein UST5r			
1369493_at	89.1	62.1	1.4	Prlr	prolactin receptor			
1368575_at	88.9	70.0	1.3	Slc6a18	solute carrier family 6 (neurotransmitter transporter), member 18			
1370824_at	88.2	60.3	1.5	Slc38a3	solute carrier family 38, member 3			
1387382_at	88.0	42.0	2.1	Hnmt	histamine N-methyltransferase			
1387303_at	83.1	59.2	1.4	Slc22a2	solute carrier family 22 (organic cation transporter), member 2			
1378247_at	81.5	41.3	2.0	Eaf2	ELL associated factor 2			
1373990_at	78.5	24.0	3.3	Slc7a12_predicted /// LOC361914	solute carrier family 7 (cationic amino acid transporter, y+ system), member 12 (predicted) /// similar to solute carrier family 7 (cationic amino acid transporter, y+ system), member 12			
1389756_at	78.0	57.9	1.3	Melk_predicted	maternal embryonic leucine zipper kinase (predicted)			
1384775_s_at	74.6	51.7	1.4	Tmprss8	transmembrane protease, serine 8 (intestinal)			
1370384_a_at	73.9	60.3	1.2	Prlr	prolactin receptor			
1368208_at	72.9	60.3	1.2	Cml1	camello-like 1			
1376944_at	72.5	68.6	1.1	Prlr	Prolactin receptor			
1385132_at	69.0	32.5	2.1	Mybl1_predicted	myeloblastosis oncogene-like 1 (predicted)			
1368651_at	66.4	49.0	1.4	Pklr	pyruvate kinase, liver and RBC			
1368304_at	65.8	57.1	1.2	Fmo3	Flavin containing monooxygenase 3			
1397205_at	54.9	42.8	1.3	Dhrs7_predicted /// LOC500672	dehydrogenase/reductase (SDR family) member 7 (predicted) /// similar to Down-regulated in nephrectomized rat kidney #3			

Table 4. Continued.

Probe sets	medulla/ papilla	cortex/ papilla	medulla/ cortex	GENE_SYMBOL	GENE_NAME	channel transporter	Metabolic enzymes	cytoskeleton /extracellular matrix
1398612_at	51.8	37.6	1.4	Akr1c12_predicted	aldo-keto reductase family 1, member C12 (predicted)			
1384639_at	51.6	49.0	1.1	Dpl1l_predicted	deleted in polyposis 1-like 1 (predicted)			
1368627_at	49.7	35.7	1.4	Rgn	regucalcin			
1368366_at	47.1	42.1	1.1	Cml2	Camello-like 2			
1387234_at	44.2	42.4	1.0	Azgp1	alpha-2-glycoprotein 1, zinc			
1368163_at	43.3	43.2	1.0	Dpp4	dipeptidylpeptidase 4			
1372841_at	41.7	32.3	1.3	Dpl1l_predicted	deleted in polyposis 1-like 1 (predicted)			
1398255_at	38.7	20.9	1.8	Slc15a2	solute carrier family 15 (H+/peptide transporter), member 2			
1367905_at	38.2	29.7	1.3	Enpp3	ectonucleotide pyrophosphatase/phosphodiesterase 3			
1370688_at	33.0	27.8	1.2	Gclc	glutamate-cysteine ligase, catalytic subunit			
1368374_a_at	31.9	29.2	1.1	Ggt1	gamma-glutamyltransferase 1			
1387218_at	30.2	23.1	1.3	Tff3	trefoil factor 3			
1370714_a_at	30.0	17.1	1.8	Siat1	sialyltransferase 1			
1373773_at	29.4	25.3	1.2	Gpm6a	glycoprotein m6a			
1387357_at	28.1	24.8	1.1	Tmlhe	trimethyllysine hydroxylase, epsilon			
1380962_at	27.6	23.3	1.2	Ace2	Angiotensin I converting enzyme (peptidyl-dipeptidase A) 2			
1370144_at	26.9	18.1	1.5	Gtpbp4 /// LOC364763 /// LOC498786	G protein-binding protein CRFG /// similar to GTP-binding protein NGB /// similar to GTP-binding protein NGB			
1387209_at	24.6	22.3	1.1	Rgpr	regucalcin gene promotor region related protein			
1367838_at	24.5	17.9	1.4	Cth	CTL target antigen			
1390855_at	23.9	12.7	1.9	Prep	Prolyl endopeptidase			
1371913_at	23.4	11.8	2.0	Tgfbi	transforming growth factor, beta induced			
1368234_at	23.4	12.1	1.9	Prep	prolyl endopeptidase			
1388145_at	22.5	22.4	1.0	Tnxa	tenascin XA			
1370365_at	22.3	14.3	1.6	Gss	glutathione synthetase			
1381350_at	20.3	17.4	1.2	Idb4	inhibitor of DNA binding 4			
1394022_at	18.0	11.8	1.5	Idb4	inhibitor of DNA binding 4			
1368164_at	17.9	14.7	1.2	Blvra	biliverdin reductase A			
1379300_at	17.5	17.0	1.0	Chst2_predicted	carbohydrate sulfotransferase 2 (predicted)			
1387296_at	17.1	15.7	1.1	Cyp2j4	cytochrome P450, family 2, subfamily J, polypeptide 4			
1377408_at	16.9	16.2	1.0	Pla2g6	phospholipase A2, group VI			
1369407_at	16.8	10.4	1.6	Tnfrsf11b	tumor necrosis factor receptor superfamily, member 11b (osteoprotegerin)			
1382868_at	16.5	9.9	1.7	Sema6a_predicted	sema domain, transmembrane domain (TM), and cytoplasmic domain, (semaphorin) 6A (predicted)			
1387819_at	16.3	16.3	1.0	Ela1	elastase 1, pancreatic			
1372523_at	16.3	14.9	1.1	Gclc	glutamate-cysteine ligase, catalytic subunit			

Table 4. Continued.

Probe sets	medulla/ papilla	cortex/ papilla	medulla/ cortex	GENE_SYMBOL	GENE_NAME	channel transporter	Metabolic enzymes	cytoskeleton /extracellular matrix
1387941_s_at	16.1	14.6	1.1	Pla2g6	phospholipase A2, group VI			
1372750_at	3.7	0.2	15.9	Fst	Follistatin			
1370072_at	15.6	12.1	1.3	Mme	membrane metallo endopeptidase			
1387966_at	15.5	11.4	1.4	Asrgl1	asparaginase-like sperm autoantigen			
1384831_at	15.1	11.7	1.3	Slc7a13_predicted	solute carrier family 7, (cationic amino acid transporter, y+ system) member 13 (predicted)			
1368189_at	14.8	11.3	1.3	Dhcr7	7-dehydrocholesterol reductase			
1367798_at	14.5	11.2	1.3	Ahcy	S-adenosylhomocysteine hydrolase			
1371059_at	14.5	14.4	1.0	Prkar2a	protein kinase, cAMP-dependent, regulatory, type 2, alpha			
1369158_at	14.4	14.3	1.0	Casr	calcium-sensing receptor			
1370030_at	14.1	11.5	1.2	Gclm	glutamate cysteine ligase, modifier subunit			
1398350_at	14.0	12.9	1.1	Basp1	brain abundant, membrane attached signal protein 1			
1369728_at	13.7	10.7	1.3	Hist1h4m_predicted	histone 1, H4m (predicted)			
1387223_at	13.6	12.2	1.1	Aadat	aminoadipate aminotransferase			
1370529_a_at	12.8	7.7	1.7	Pld1	phospholipase D1			
1384603_at	12.8	9.8	1.3	Abca4_predicted	ATP-binding cassette, sub-family A (ABC1), member 4 (predicted)			
1369494_a_at	12.0	6.6	1.8	Ghrhr	growth hormone releasing hormone receptor			
1367729_at	11.9	11.4	1.0	Oat	ornithine aminotransferase			
1374565_at	11.8	9.7	1.2	Nek6	NIMA (never in mitosis gene a)-related expressed kinase 6			
1368431_at	11.6	10.3	1.1	Hpn	hepsin			
1382274_at	11.5	5.5	2.1	Rarres1_predicted	retinoic acid receptor responder (tazarotene induced) 1 (predicted)			
1374871_at	11.2	7.3	1.5	Asrgl1	asparaginase-like sperm autoantigen			
1392965_a_at	11.0	2.3	4.8	Smoc2_predicted	SPARC related modular calcium binding 2 (predicted)			
1370163_at	11.0	6.5	1.7	Odc1	ornithine decarboxylase 1			
1390208_at	10.7	10.7	1.0	Htatip2_predicted	HIV-1 Tat interactive protein 2 (predicted)			
1370530_a_at	10.6	5.7	1.9	Pld1	phospholipase D1			
1376852_at	10.5	8.3	1.3	Mccc1_predicted	methylcrotonoyl-Coenzyme A carboxylase 1 (alpha) (predicted)			
1369184_at	10.5	6.8	1.5	Cldn16	claudin 16			
1385970_at	10.4	9.5	1.1	Sh2bp1_predicted	SH2 domain binding protein 1 (tetratricopeptide repeat containing) (predicted)			
1383742_at	10.1	9.4	1.1	Snx7_predicted	sorting nexin 7 (predicted)			

After selection by ANOVA ($p<0.01$) for the data of percellome normalization, genes maximally expressed in medulla were selected. The genes were aligned in the order of the ratio to the lower expression value, either in papilla or in cortex. As the genes listed here are expressed in medulla and cortex to a similar extent, exceptional cases (ratio >3) are shaded in the medulla/cortex column. The genes categorized to "channel/transporters", "metabolic enzymes", or "cytoskeleton/extracellular matrix" are also shaded. Proteases or enzymes involving signal transduction are not included in the category of "metabolic enzymes". For simplicity, genes with less than 10-fold specificity are omitted.

Table 5. A list of probe sets specifically expressed in cortex of kidney.

Probe sets	cortex/ papilla	medulla/ papilla	cortex/ medulla	GENE_SYMBOL	GENE_NAME	channel transporter	Metabolic enzymes	cytoskeleton /extracellular matrix
1387314_at	312.0	259.8	1.2	Sult1b1	sulfotransferase family 1B, member 1			
1387820_at	284.9	14.7	19.4	Klk7	kallikrein 7			
1388172_at	245.4	110.3	2.2	Ust1r	integral membrane transport UST1r			
1368064_a_at	230.1	19.6	11.8	Ddc	dopa decarboxylase			
1390591_at	224.2	166.1	1.3	Slc17a3	Na/Pi cotransporter 4			
1368467_at	217.1	117.6	1.8	Cyp4f2	cytochrome P450, family 4, subfamily F, polypeptide 2			
1368600_at	210.7	75.0	2.8	Slc26a1	solute carrier family 26 (sulfate transporter), member 1			
1396039_at	202.5	188.6	1.1	Slc22a12_predicted	solute carrier family 22 (organic anion/cation transporter), member 12 (predicted)			
1387230_at	193.9	13.2	14.7	Slc12a3	solute carrier family 12, member 3			
1368245_at	192.4	134.7	1.4	Upb1	ureidopropionase, beta			
1367917_at	192.3	124.6	1.5	Cyp2d26	cytochrome P450, family 2, subfamily d, polypeptide 26			
1367871_at	187.8	32.3	5.8	Cyp2e1	cytochrome P450, family 2, subfamily e, polypeptide 1			
1376267_at	185.1	13.9	13.4	Slc16a6	Solute carrier family 16 (monocarboxylic acid transporters), member 6			
1384877_at	183.4	73.9	2.5	Aqp11	aquaporin 11			
1398282_at	174.5	75.2	2.3	Kynu	kynureninase (L-kynurenine hydrolase)			
1370547_at	169.5	56.4	3.0	Pzp	pregnancy-zone protein			
1368563_at	149.7	96.7	1.5	Aspa	aspartoacylase			
1383111_at	149.3	60.1	2.5	Acmsd	2-amino-3-carboxymuconate-6-semialdehyde decarboxylase			
1370991_at	146.7	32.6	4.5	Cml3	camello-like 3			
1387188_at	144.5	86.8	1.7	RGD:620099	solute carrier family 17 (sodium phosphate), member 1			
1370936_at	143.4	91.3	1.6	Dmgdh	dimethylglycine dehydrogenase precursor			
1367804_at	142.8	21.8	6.5	Sap	serum amyloid P-component			
1368915_at	141.5	87.2	1.6	Kmo	kynurenine 3-monooxygenase (kynurenine 3-hydroxylase)			
1398511_at	138.7	16.8	8.3	Susd2_predicted	sushi domain containing 2 (predicted)			
1387851_at	129.9	78.3	1.7	Pter	phosphotriesterase related			
1376051_at	127.0	63.2	2.0	Cryl1	crystallin, lamda 1			
1384112_at	125.1	80.6	1.6	Nt5	5 nucleotidase			
1393894_at	123.8	94.1	1.3	RGD:628846	cytochrome P450, 4a12			
1370725_a_at	116.9	15.4	7.6	G6pc	glucose-6-phosphatase, catalytic			
1386980_at	116.6	64.2	1.8	Apom	apolipoprotein M			
1377125_at	116.3	28.0	4.2	Dnajc6_predicted	DnaJ (Hsp40) homolog, subfamily C, member 6 (predicted)			
1368317_at	114.8	70.5	1.6	Aqp7	aquaporin 7			
1370615_at	114.4	28.0	4.1	RGD:708417	UDP-glucuronosyltransferase			

Table 5. Continued.

Probe sets	cortex/ papilla	medulla/ papilla	cortex/ medulla	GENE_SYMBOL	GENE_NAME	channel transporter	Metabolic enzymes	cytoskeleton /extracellular matrix
1368236_at	113.4	105.5	1.1	Mep1a	meprin 1 alpha			
1373386_at	113.2	110.8	1.0	Gjb2	gap junction membrane channel protein beta 2			
1369636_at	112.6	41.2	2.7	Sord	sorbitol dehydrogenase			
1368521_at	110.8	46.3	2.4	Napsa	napsin A aspartic peptidase			
1368150_at	110.4	78.2	1.4	Slc27a2 /// LOC497779	solute carrier family 27 (fatty acid transporter), member 2 /// hypothetical gene supported by NM_031736			
1369635_at	109.5	42.4	2.6	Sord	sorbitol dehydrogenase			
1368180_s_at	107.9	73.9	1.5	Gsta2	glutathione-S-transferase, alpha type2			
1368190_at	105.6	12.1	8.7	Ren1	renin 1			
1377051_at	104.7	17.9	5.8	Mpv17l_predicted	Mpv17 transgene, kidney disease mutant-like (predicted)			
1387336_at	102.7	89.7	1.1	Nat8	*N*-acetyltransferase 8 (camello like)			
1387631_at	102.4	59.8	1.7	Hpgd	15-hydroxyprostaglandin dehydrogenase			
1379885_at	100.7	91.4	1.1	Fmo4	flavin containing monooxygenase 4			
1368659_at	100.0	60.0	1.7	Agxt2	alanine-glyoxylate aminotransferase 2			
1370259_a_at	99.6	31.1	3.2	Pthr1	parathyroid hormone receptor 1			
1368188_at	94.6	25.6	3.7	Hpd	4-hydroxyphenylpyruvic acid dioxygenase			
1369200_at	93.4	56.3	1.7	Nt5	5 nucleotidase			
1387053_at	90.3	37.7	2.4	Fmo1	flavin containing monooxygenase 1			
1388569_at	88.3	50.7	1.7	Serpinf1	serine (or cysteine) proteinase inhibitor, clade F), member 1			
1390857_at	87.5	26.6	3.3	Xylb_predicted	xylulokinase homolog (H. influenzae) (predicted)			
1387375_at	86.9	64.4	1.4	Khk	ketohexokinase			
1387034_at	86.3	17.7	4.9	Pah	phenylalanine hydroxylase			
1397740_at	86.3	51.0	1.7	Sfxn1_predicted	sideroflexin 1 (predicted)			
1368736_at	84.2	18.9	4.4	Tsx	testis specific X-linked gene			
1398514_at	82.6	81.3	1.0	Hgd_predicted	homogentisate 1, 2-dioxygenase (predicted)			
1368515_at	81.1	7.2	11.3	Epb4.1l3	erythrocyte protein band 4.1-like 3			
1368794_at	81.0	78.4	1.0	Haao	3-hydroxyanthranilate 3,4-dioxygenase			
1370964_at	80.8	27.0	3.0	Ass	arginosuccinate synthetase			
1368077_at	79.6	43.0	1.9	Fbp1	fructose-1,6- biphosphatase 1			
1370397_at	77.6	68.8	1.1	Cyp4a14	cytochrome P450, family 4, subfamily a, polypeptide 14			
1368397_at	76.3	36.6	2.1	Ugt2b5 /// Ugt2b4	UDP-glucuronosyltransferase 2 family, member 5 /// UDP glycosyltransferase 2 family, polypeptide B4			
1368282_at	74.3	24.9	3.0	Dpep1	dipeptidase 1 (renal)			
1395026_at	73.7	59.0	1.2	Fmo4	flavin containing monooxygenase 4			
1380577_at	70.1	53.6	1.3	Abcg2	ATP-binding cassette, sub-family G (WHITE), member 2			

Table 5. Continued.

Probe sets	cortex/ papilla	medulla/ papilla	cortex/ medulla	GENE_SYMBOL	GENE_NAME	channel transporter	Metabolic enzymes	cytoskeleton /extracellular matrix
1387339_at	69.4	19.2	3.6	Sepp1	selenoprotein P, plasma, 1			
1382913_at	68.9	16.8	4.1	Cttnbp2	cortactin binding protein 2			
1376327_at	68.9	24.2	2.8	Tnfrsf14_predicted	tumor necrosis factor receptor superfamily, member 14 (herpesvirus entry mediator) (predicted)			
1368178_at	66.6	32.4	2.1	Pdzk1	PDZ domain containing 1			
1377672_at	66.3	37.3	1.8	Sult1c2	sulfotransferase family, cytosolic, 1C, member 2			
1387084_at	65.5	55.5	1.2	Dpp4	dipeptidylpeptidase 4			
1374512_at	63.7	35.5	1.8	Cdh7	Cadherin 7, type 2			
1371824_at	63.6	40.8	1.6	Ak3l1	adenylate kinase 3-like 1			
1369412_a_at	63.4	37.9	1.7	Slc19a1	solute carrier family 19, member 1			
1373803_a_at	63.1	39.2	1.6	Ghr	growth hormone receptor			
1387259_at	62.9	29.4	2.1	Cdh2 /// LOC497718	cadherin 2 /// hypothetical gene supported by NM_031333			
1389166_at	62.8	31.1	2.0	Cib2_predicted	calcium and integrin binding family member 2 (predicted)			
1371354_at	62.1	8.0	7.8	Tncc_predicted	troponin C, cardiac/slow skeletal (predicted)			
1372672_at	58.8	36.8	1.6	Qprt_predicted	quinolinate phosphoribosyltransferase (predicted)			
1369491_at	58.4	36.1	1.6	Dao1	D-amino acid oxidase			
1387111_at	57.3	33.4	1.7	Ddah1	dimethylarginine dimethylaminohydrolase 1			
1367988_at	57.1	22.1	2.6	Cyp2c23	cytochrome P450, family 2, subfamily c, polypeptide 23			
1368607_at	56.5	51.1	1.1	RGD:628846	cytochrome P450, 4a12			
1370881_at	55.8	22.9	2.4	Tst	thiosulfate sulfurtransferase			
1369259_at	55.6	28.4	2.0	Dio1	deiodinase, iodothyronine, type I			
1376709_at	55.2	42.5	1.3	Slc39a8_predicted	solute carrier family 39 (metal ion transporter), member 8 (predicted)			
1387013_at	55.2	27.3	2.0	Tmem27	kidney-specific membrane protein			
1387808_at	54.9	5.1	10.8	Slc7a7	solute carrier family 7 (cationic amino acid transporter, y+ system), member 7			
1368283_at	54.7	29.8	1.8	Ehhadh	enoyl-Coenzyme A, hydratase/3-hydroxyacyl Coenzyme A dehydrogenase			
1373337_at	53.4	22.5	2.4	Grhpr_predicted	glyoxylate reductase/hydroxypyruvate reductase (predicted)			
1383654_a_at	53.2	14.7	3.6	Fnsk	similar to fructosamine-3-kinase			
1368924_at	51.8	42.4	1.2	Ghr	growth hormone receptor			
1368092_at	50.7	35.9	1.4	Fah	fumarylacetoacetate hydrolase			
1380171_at	49.4	39.5	1.3	Adra2b	Adrenergic receptor, alpha 2b			
1367952_at	45.8	26.5	1.7	Lrp2	low density lipoprotein receptor-related protein 2			

Table 5. Continued.

Probe sets	cortex/ papilla	medulla/ papilla	cortex/ medulla	GENE_SYMBOL	GENE_NAME	channel transporter	Metabolic enzymes	cytoskeleton /extracellular matrix
1369705_at	44.1	42.6	1.0	RGD:621651	X transporter protein 3			
1368680_a_at	43.6	25.3	1.7	Slc34a1	solute carrier family 34 (sodium phosphate), member 1			
1367627_at	43.5	14.8	2.9	Gatm	glycine amidinotransferase (L-arginine:glycine amidinotransferase)			
1379950_at	42.9	37.7	1.1	Cml2	Camello-like 2			
1367775_at	42.6	32.3	1.3	Amacr	alpha-methylacyl-CoA racemase			
1388176_at	42.4	24.0	1.8	Cml5	camello-like 5			
1368322_at	42.1	8.2	5.1	Sod3	superoxide dismutase 3, extracellular			
1372264_at	42.1	15.9	2.7	Pck1	phosphoenolpyruvate carboxykinase 1			
1397647_at	41.9	17.1	2.5	Slc25a15_predicted	solute carrier family 25 (mitochondrial carrier; ornithine transporter) member 15 (predicted)			
1369073_at	41.9	12.2	3.4	Nr1h4	nuclear receptor subfamily 1, group H, member 4			
1368877_at	41.6	13.7	3.0	Znf354a	zinc finger protein 354A			
1390119_at	41.4	4.9	8.4	Sfrp2	secreted frizzled-related protein 2			
1367774_at	41.1	31.8	1.3	Gsta5	glutathione S-transferase A5			
1376191_at	40.1	27.6	1.5	Hpgd	15-hydroxyprostaglandin dehydrogenase			
1397526_at	39.3	23.5	1.7	Gcdh_predicted	glutaryl-Coenzyme A dehydrogenase (predicted)			
1374384_at	38.8	16.3	2.4	Crygc	Crystallin, gamma C			
1387491_at	38.5	10.9	3.5	Gyk	glycerol kinase			
1386944_a_at	38.3	7.7	5.0	G6pc	glucose-6-phosphatase, catalytic			
1367999_at	37.7	22.6	1.7	Aldh2	aldehyde dehydrogenase 2			
1369182_at	37.6	9.6	3.9	F3	coagulation factor 3			
1382975_at	37.4	20.8	1.8	Ceacam1	CEA-related cell adhesion molecule 1			
1374200_at	36.1	16.7	2.2	Slc29a3	solute carrier family 29 (nucleoside transporters), member 3			
1369973_at	35.6	9.6	3.7	Xdh /// LOC497811	xanthine dehydrogenase /// hypothetical gene supported by NM_017154			
1372306_at	35.4	22.9	1.5	Ethe1_predicted	ethylmalonic encephalopathy 1 (predicted)			
1370818_at	34.6	12.5	2.8	Decr2	2-4-dienoyl-Coenzyme A reductase 2, peroxisomal			
1397797_at	33.3	29.3	1.1	Tigd3	Tigger transposable element derived 3 (predicted)			
1372323_at	32.9	23.4	1.4	Sardh	sarcosine dehydrogenase			
1368412_a_at	32.5	5.3	6.1	Ptpro	protein tyrosine phosphatase, receptor type, O			
1390036_at	32.5	6.0	5.4	Slc16a6	solute carrier family 16 (monocarboxylic acid transporters), member 6			
1397744_at	32.5	22.2	1.5	Sardh	Sarcosine dehydrogenase			
1368642_at	32.4	19.5	1.7	Cdh2 /// LOC497718	cadherin 2 /// hypothetical gene supported by NM_031333			
1373188_at	32.0	12.2	2.6	Scn4b	sodium channel, voltage-gated, type IV, beta			